Applied Physics B (2024) 130:175
https://doi.org/10.1007/s00340-024-08310-0

RESEARCH

Analysis of the process $e^+e^- \rightarrow \mu^+\mu^-$ in the presence of a linearly polarized electromagnetic field

M. Ouali[1] · M. Ouhammou[1] · M. Jakha[1] · S. Taj[1] · B. Manaut[1]

Received: 12 April 2024 / Accepted: 26 August 2024

Abstract

In the centre of mass frame, we have investigated the electroweak process $e^+e^- \rightarrow \mu^+\mu^-$ in the presence of a plane and monochromatic laser wave of linear polarization. We provide the theoretical calculations of the differential cross-section for this process by using the scattering-matrix approach and Dirac-Volkov formalism. The laser-assisted cross-section is computed, and its dependence on the laser parameters is analyzed. We have found that this cross-section increases significantly inside a linearly polarized laser wave co-propagating with the incident particle's beam, and it passes its corresponding laser-free cross-section by several orders of magnitude.

1 Introduction

Laser physics is one of the most exciting and challenging fields in physics. Since the invention of the laser in 1960 [1] till today, a great progress has been made in this field of physics both theoretically and experimentally. Lasers are useful as they are indispensable tools in different fields of physics such as optics, medical physics, biology, nuclear physics, etc. Radiation-matter interactions have received a great interest from both theoretical and experimental physicists [2–8]. In atomic physics, several research papers have been published in non-relativistic and relativistic regimes. Then, some researchers included the electromagnetic field interactions in elementary particle decay [9–13] and scattering reactions, especially those of e^+e^- collisions [14–23]. In general, the process of e^+e^- annihilation into a pair of fermions can proceed in both resonant and non-resonant manner. Under resonance conditions, the intermediate propagator is on the mass shell. These resonance phenomena are known as Oleinik resonances, and they have been studied very extensively by Roshchupkin et al in enormous and high quality papers such as laser-assisted processes in Quantum Electrodynamics (QED) (see the following references [24–32] for more details). In the present paper, we consider the non-resonant case, where the intermediate particles are considered as virtual bosons. The process of muon pair production via e^+e^- collision inside an external field is studied in quantum electrodynamics (QED) for both linear [33] and circular [34] polarization of the laser field. However, at high energies, the interference between the γ-photon contribution and Z-boson exchange are both important. Therefore, we studied in references [35, 36] the process $e^+e^- \rightarrow \mu^+\mu^-$ at the leading order by taking into consideration both γ-photon and Z-boson exchange in the presence of a laser field with circular polarization. In these papers, we have found that laser wave with circular polarization reduces the probability of the process to occur; its cross-section is decreased by the circularly polarized electromagnetic field. However, as this process is an elementary and fundamental process for other e^+e^- collisions, it is important to look for ways that lead to the enhancement of its cross section. In addition, we assume that the polarization of the laser may be crucial for the cross-section's behavior. In this respect, we investigate in this paper this electroweak process inside an electromagnetic wave of linear polarization. Further, by analyzing numerical data obtained from the theoretical calculations, we illustrate the effect of the linearly polarized laser field on the process's cross section.

The remained of this paper is structured as follows: In the next section, we present a detailed analytic calculation of the cross-section of the process $e^+e^- \rightarrow \mu^+\mu^-$ inside a linearly polarized laser wave. Then, we compute this cross-section and analyze the obtained results. Finally, a short conclusion is given in the last section.

✉ M. Ouali
mohaa.oualii@gmail.com

[1] Research Laboratory in Physics and Engineering Sciences, Team of Modern and Applied Physics, FPBM, USMS, Morocco

Published online: 11 September 2024

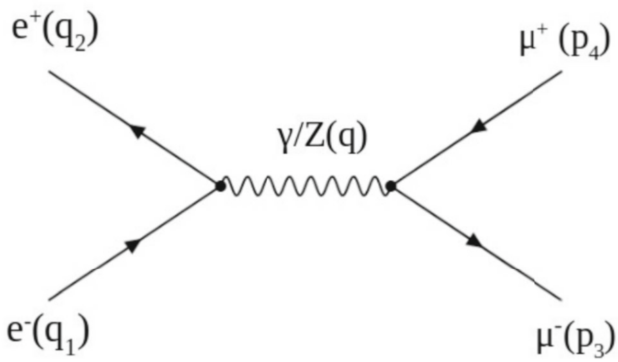

Fig. 1 Feynman diagrams of the process $e^+e^- \to \mu^+\mu^-$

2 Theoretical calculation

We consider, in this part, the cross-section of the muon-antimuon pair creation from electron-positron collisions inside an electromagnetic field with linear polarization. We adopt natural units ($\hbar = c = 1$), the Livi-Civita tensor $\epsilon^{0123} = 1$ and the metric $g^{\mu\nu} = (1, -1, -1, -1)$. The Z-boson and γ photon interference are taken into consideration, and the Feynman diagrams for this process are depicted in Fig. 1.

According to the Feynman rules, the laser-assisted scattering matrix element of this process can be expressed as follows:

$$S_{fi}(e^+e^- \to \mu^+\mu^-) = \int\int \Big\{ J^{\mu}_{e^+e^-Z}(x) D_{\mu\nu}(x-y) J^{\nu}_{Z\mu^+\mu^-}(y) + J^{\mu}_{e^+e^-\gamma}(x) G_{\mu\nu}(x-y) J^{\nu}_{\gamma\mu^+\mu^-}(y) \Big\} d^4x d^4y, \quad (1)$$

where the currents of the incoming particles coupling to Z-boson and γ photon are expressed as follows:

$$\begin{cases} J^{\mu}_{e^+e^-Z}(x) = \overline{\psi}_{p_2,s_2}(x) \dfrac{i\,g}{4\cos\theta_W}\gamma^{\mu}(g_v - g_a\gamma^5)\psi_{p_1,s_1}(x) \\ J^{\mu}_{e^+e^-\gamma}(x) = \overline{\psi}_{p_2,s_2}(x)(ie\gamma^{\mu})\psi_{p_1,s_1}(x). \end{cases} \quad (2)$$

Similarly, the currents of the outgoing particles are given by:

$$\begin{cases} J^{\nu}_{Z\mu^+\mu^-}(y) = \overline{\psi}_{p_3,s_3}(y) \dfrac{i\,g}{4\cos\theta_W}\gamma^{\nu}(g_v - g_a\gamma^5)\psi_{p_4,s_4}(y) \\ J^{\nu}_{\gamma\mu^+\mu^-}(y) = \overline{\psi}_{p_3,s_3}(y)(ie\gamma^{\nu})\psi_{p_4,s_4}(y), \end{cases} \quad (3)$$

with ψ_{p_1,s_1}, ψ_{p_2,s_2}, ψ_{p_3,s_3} and ψ_{p_4,s_4} are successively the states of the incident electron, incident positron, outgoing muon and outgoing antimuon. θ_W is the Weinberg angle, $g = e/\sin\theta_W$ the electroweak coupling constant, and the leptonic weak neutral coupling constants $g_v = -1 + 4\sin^2\theta_W$ and $g_a = -1$. The propagators of the Z-boson and the γ photon [37] are successively given by the following expressions:

$$D_{\mu\nu}(x-y) = \int \frac{d^4q}{(2\pi)^4}\frac{e^{-iq(x-y)}}{q^2 - M_Z^2}\Big(-ig_{\mu\nu} + i\frac{q_\mu q_\nu}{M_Z^2}\Big), \quad (4)$$

$$G_{\mu\nu}(x-y) = \int \frac{d^4q}{(2\pi)^4}\frac{e^{-iq(x-y)}}{q^2}\Big(-ig_{\mu\nu} + i\frac{q_\mu q_\nu}{q^2}\Big), \quad (5)$$

with q denoting their four-momentum. The incoming electron and positron, which are charged fermions, are embedded in a laser field. Therefore, their states are derived from Dirac equation, $(i\partial\!\!\!/ - eA\!\!\!/ - m)\psi_e(x) = 0$, as follows [39]

$$\begin{cases} \psi_{p_1,s_1}(x) = \Big[1 - \dfrac{e k\!\!\!/ A\!\!\!/}{2(k.p_1)}\Big]\dfrac{u(p_1,s_1)}{\sqrt{2Q_1V}}e^{iS(q_1,s_1)} \\ \psi_{p_2,s_2}(x) = \Big[1 + \dfrac{e k\!\!\!/ A\!\!\!/}{2(k.p_2)}\Big]\dfrac{v(p_2,s_2)}{\sqrt{2Q_2V}}e^{iS(q_2,s_2)}, \end{cases} \quad (6)$$

where the classical actions $S(q_i, s_i)(i = 1, 2)$ are defined as:

$$\begin{cases} S(q_1, s_1) = -q_1x + \frac{e(\xi_l.p_1)}{k.p_1}\sin\phi - \frac{e^2\xi_l^2}{8(k.p_1)}\sin 2\phi \\ S(q_2, s_2) = +q_2x + \frac{e(\xi_l.p_2)}{k.p_2}\sin\phi + \frac{e^2\xi_l^2}{8(k.p_2)}\sin 2\phi \end{cases}. \quad (7)$$

V is the quantization volume. The free Dirac spinors $u_{(p_1,s_1)}$ and $v_{(p_2,s_2)}$ are fulfilling the normalization: $\sum_{s_i} u(p_i, s_i)\bar{u}(p_i, s_i) = p\!\!\!/_i + m_e$ for particle and $\sum_{s_i} v(p_i, s_i)\bar{v}(p_i, s_i) = p\!\!\!/_i - m_e$ for antiparticle, with s_i denotes the particle's spin, and x is the space-time coordinate of the incident particles. $q_1(Q_1, \vec{q}_1)$ and $q_2(Q_2, \vec{q}_2)$ are their effective four-momenta acquired inside a laser field. In the centre of mass frame, the free four-momenta of the electron and positron outside the electromagnetic field are expressed by: $p_1 = (E_1, |\mathbf{p_1}|, 0, 0)$ and $p_2 = (E_2, -|\mathbf{p_2}|, 0, 0)$. The free-momentum and its corresponding effective momentum are related by the following equation:

$$q_i^{\mu} = p_i^{\mu} + \frac{e^2\xi_l^2}{4(k.p_i)}k^{\mu}, \qquad i = (1, 2). \quad (8)$$

Since the Dirac-Volkov states of the incident electron and positron (Eq. 6) depend on the electromagnetic potential A^{μ} ($A\!\!\!/ = A^{\mu}\gamma_{\mu}$), the polarization of the laser field has an important role in the evolution of the transition amplitude. In this paper, we assume that the laser field is linearly polarized, and its classical potential is read as:

$$A_l^{\mu}(\phi) = \xi_l^{\mu}\cos(\phi), \quad (9)$$

where $\xi_l^\mu = (0, 0, |\xi|, 0)$ is the polarization 4-vector with $\xi_l^2 = |\xi|^2 = (\varepsilon/\omega)^2$, and ε is the amplitude of the laser field. $\phi = (k.x)$ is the phase of the electromagnetic field, and k^μ is its wave four-vector such that $k^\mu = (\omega, \omega, 0, 0)$ satisfying $(\xi_l.k) = 0$ with ω denotes the laser frequency. Since the produced muon and antimuon are much heavier than electron and positron ($m_\mu \approx 200 m_e$), they will not interact with the laser field unless its strength overcomes $\varepsilon = 10^{10} V.cm^{-1}$ [35]. In this paper, we consider laser strength less than this limit. Therefore, we describe them as free states [37] such that:

$$\begin{cases} \psi_{p_3,s_3}(y) = \frac{u(p_3,s_3)}{\sqrt{2E_3V}} e^{-ip_3y} \\ \psi_{p_4,s_4}(y) = \frac{v(p_4,s_4)}{\sqrt{2E_4V}} e^{+ip_4y}. \end{cases} \tag{10}$$

The free-momentum of the outgoing particles in the centre of mass frame are expressed as $p_3 = (E_3, |\mathbf{p_3}|\cos\theta, |\mathbf{p_3}|\sin\theta, 0)$ and $p_4 = (E_4, -|\mathbf{p_4}|\cos\theta, -|\mathbf{p_4}|\sin\theta, 0)$, with $E_i (i = 3, 4)$ are their energies. To evaluate the S-matrix element given by Eq. (1), we have to replace the particles' states and the Z and γ-propagators by their expressions. After simplification, the scattering matrix element will be as follows:

$$\begin{aligned} S_{fi} = &\sum_{n=-\infty}^{+\infty} \frac{(2\pi)^4\delta^4(p_3+p_4-q_1-q_2-nk)}{4V^2\sqrt{Q_1Q_2E_3E_4}} \\ &\Bigg\{\frac{g^2}{4\cos^2\theta_W}\frac{1}{(q_1+q_2+nk)^2} \\ &\times\Bigg[\bar{u}(p_3,s_3)\gamma^\mu(g_v^e - g_a^e\gamma^5)v(p_4,s_4)\bar{v}(p_2,s_2) \\ &\Big[C_0B_{0n} + C_1B_{1n} + C_2B_{2n}\Big]u(p_1,s_1)\Bigg] \\ &+\frac{e^2}{(q_1+q_2+nk)^2} \\ &\Bigg[\bar{u}(p_3,s_3)\gamma^\mu v(p_4,s_4)\bar{v}(p_2,s_2) \\ &\Big[D_0B_{0n} + D_1B_{1n} + D_2B_{2n}\Big]u(p_1,s_1)\Bigg]\Bigg\} \\ = &\sum_{n=-\infty}^{+\infty} S_{fi}^n, \end{aligned} \tag{11}$$

where S_{fi}^n and S_{fi} are successively the partial and total scattering matrix elements. The parameter n is interpreted as a number of emitted (if $n < 0$) or absorbed photons (if $n > 0$). The quantities $C_{0,1,2}$ and $D_{0,1,2}$ are explicitly expressed by:

$$\begin{cases} C_0 = \gamma^\mu(g_v^e - g_a^e\gamma^5) \\ C_1 = cp_2\not{\xi}_l\not{k}\gamma^\mu(g_v^e - g_a^e\gamma^5) - cp_1\gamma^\mu(g_v^e - g_a^e\gamma^5)\not{k}\not{\xi}_l \\ C_2 = cp_1cp_2\not{\xi}_l\not{k}\gamma^\mu(g_v^e - g_a^e\gamma^5)\not{k}\not{\xi}_l \end{cases};$$

$$\begin{cases} D_0 = \gamma^\mu \\ D_1 = cp_2\not{\xi}_l\not{k}\gamma^\mu - cp_1\gamma^\mu\not{k}\not{\xi}_l \\ D_2 = cp_1cp_2\not{\xi}_l\not{k}\gamma^\mu\not{k}\not{\xi}_l \end{cases}. \tag{12}$$

Besides, the coefficients B_{0n}, B_{1n} and B_{2n} are expressed in terms of generalized Bessel functions by:

$$\begin{cases} B_{0n} = J_n(\alpha_1, \alpha_2) \\ B_{1n} = \frac{1}{2}\Big(J_{n-1}(\alpha_1,\alpha_2) + J_{n+1}(\alpha_1,\alpha_2)\Big) \\ B_{2n} = \frac{1}{4}\Big(J_{n-2}(\alpha_1,\alpha_2) + 2J_n(\alpha_1,\alpha_2) + J_{n+2}(\alpha_1,\alpha_2)\Big). \end{cases} \tag{13}$$

Here, we use the generalized Bessel functions [38], which are composed of products of regular cylindrical Bessel functions,

$$J_n(\alpha_1, \alpha_2) = \sum_{n'=-\infty}^{+\infty} J_{n-2n'}(\alpha_1)J_{n'}(\alpha_2), \tag{14}$$

with

$$\alpha_1 = e\Big[\frac{\xi_l.p_2}{k.p_2} - \frac{\xi_l.p_1}{k.p_1}\Big];\ \alpha_2 = \frac{e^2\xi_l^2}{8}\Big[\frac{1}{k.p_2} + \frac{1}{k.p_1}\Big]. \tag{15}$$

The product $\xi_l.p_i = 0$, hence $\alpha_1 = 0$. Thus, the sum in the generalized Bessel functions collapses and the inner summation index n' is fixed at $n' = n/2$ such that:

$$\begin{aligned} J_n(\alpha_1,\alpha_2) &= \sum_{n'=-\infty}^{+\infty} J_{n-2n'}(\alpha_1)J_{n'}(\alpha_2) \\ &= \sum_{n'=-\infty}^{+\infty} J_{n-2n'}(0)J_{n'}(\alpha_2) \\ &= J_{n/2}(\alpha_2). \end{aligned} \tag{16}$$

Since the regular Bessel function $J_{n'}(\alpha_2)$ must be of integer order, n must be even and thus only pairs of laser photons are absorbed or emitted at the electron-positron vertex. To obtain the differential cross-section in the centre of mass frame, we divide the square of the scattering matrix element by VT to obtain the transition probability per volume, then by J_{inc} and by the particle density $\rho = V^{-1}$. Finally, we integrate over the final states for a fixed emission angle $d\Omega = \sin\theta d\theta d\phi$ where θ is the scattering angle. The total cross-section can be expressed as follows:

$$d\sigma_n = \frac{|S_{fi}^n|^2}{VT}\frac{1}{|J_{inc}|}\frac{1}{\rho}V\int\frac{d^3p_3}{(2\pi)^3}V\int\frac{d^3p_4}{(2\pi)^3}, \tag{17}$$

where the incident current $|J_{inc}| = (\sqrt{(q_1q_2)^2 - m_e^{*4}}/Q_1Q_2V)$, and m_e^* is the effective mass of the electron and positron. Now, we have to average over the polarizations of the incoming particles, and we sum over the final ones,

$$
\begin{aligned}
& d\sigma_n(e^+e^- \to \mu^+\mu^-) \\
& = \frac{1}{16\sqrt{(q_1q_2)^2 - m_e^{*4}}} \overline{\left|M_{fi}^n\right|}^2 \int \frac{|\mathbf{p}_3|^2 d|\mathbf{p}_3| d\Omega}{(2\pi)^2 E_3} \int \frac{d^3 p_4}{E_4} \\
& \quad \times \delta^4(p_3 + p_4 - q_1 - q_2 - nk).
\end{aligned} \tag{18}
$$

In this equation, we first integrate over $d^3 p_3$, and then the integral over $d^3 p_4$ can be performed by applying the well-known formula given by [37] :

$$
\int d\mathbf{x} f(\mathbf{x}) \delta(g(\mathbf{x})) = \frac{f(\mathbf{x})}{|g^{'}(\mathbf{x})|_{g(\mathbf{x})=0}}. \tag{19}
$$

In Eq. (19), the delta function, $\delta^4(p_3 + p_4 - q_1 - q_2 - nk)$, ensures the conservation of energy and momentum through the interaction. As a result, the final expression of the partial differential cross-section becomes as follows:

$$
\begin{aligned}
& \frac{d\sigma_n}{d\Omega}(e^+e^- \to \mu^+\mu^-) \\
& = \frac{1}{16\sqrt{(q_1q_2)^2 - m_e^{*4}}} \overline{\left|M_{fi}^n\right|}^2 \frac{2|\mathbf{p}_3|^2}{(2\pi)^2 E_3} \frac{1}{|g^{'}(|\mathbf{p}_3|)|_{g(|\mathbf{p}_3|)=0}},
\end{aligned} \tag{20}
$$

where the expression of the function $g^{'}(|\mathbf{p}_3|)$ is given by:

$$
\begin{aligned}
g^{'}(|\mathbf{p}_3|) = & -2\Big[\frac{E_1|\mathbf{p}_3|}{\sqrt{|\mathbf{p}_3|^2 + m_\mu^2}} - |\mathbf{p}_1|\cos\theta\Big] \\
& - \frac{e^2\xi^2}{2k.p_1}\Big[\frac{\omega|\mathbf{p}_3|}{\sqrt{|\mathbf{p}_3|^2 + m_\mu^2}} - \omega\cos\theta\Big] \\
& -2\Big[\frac{E_2|\mathbf{p}_3|}{\sqrt{|\mathbf{p}_3|^2 + m_\mu^2}} + |\mathbf{p}_2|\cos\theta\Big] \\
& - \frac{e^2\xi^2}{2k.p_2}\Big[\frac{\omega|\mathbf{p}_3|}{\sqrt{|\mathbf{p}_3|^2 + m_\mu^2}} - \omega\cos\theta\Big] \\
& -2n\Big[\frac{\omega|\mathbf{p}_3|}{\sqrt{|\mathbf{p}_3|^2 + m_\mu^2}} - \omega\cos\theta\Big].
\end{aligned} \tag{21}
$$

In Eq. (18), the spinorial part $\left|\overline{M_{fi}^n}\right|^2$ can be evaluated as follows:

$$
\begin{aligned}
\overline{|M_{fi}^n|}^2 = & \frac{1}{4}\sum_{pol}\sum_{spins}|M_{fi}^n|^2 \\
= & \frac{1}{4}\Big\{\frac{g^4}{16\cos^4\theta_W}\Big(\frac{1}{(q_1+q_2+nk)^2 - M_Z^2}\Big)^2 \\
& \times Tr\Big[(\not{p}_3 + m_\mu)\gamma^\mu(g_v^e - g_a^e\gamma^5)(\not{p}_4 - m_\mu) \\
& \gamma_\mu(g_v^e - g_a^e\gamma^5)\Big]Tr\Big[(\not{p}_2 - m_e)\tau^n(\not{p}_1 + m_e)\overline{\tau}^n\Big] \\
& + \frac{e^4}{(q_1+q_2+nk)^4}Tr\Big[(\not{p}_3 + m_\mu)\gamma^\mu(\not{} \\
& p_4 - m_\mu)\gamma_\mu\Big]Tr\Big[(\not{p}_2 - m_e)\kappa^n(\not{p}_1 + m_e)\overline{\kappa}^n\Big] \\
& + \frac{e^2}{(q_1+q_2+nk)^2}\frac{g^2}{4\cos^2\theta_W}\Big(\frac{1}{(q_1+q_2+nk)^2 - M_Z^2}\Big) \\
& Tr\Big[(\not{p}_3 + m_\mu)\gamma^\mu(g_v^e - g_a^e\gamma^5) \\
& \times(\not{p}_4 - m_\mu)\gamma_\mu\Big]Tr\Big[(\not{p}_2 - m_e)\tau^n(\not{p}_1 + m_e)\overline{\kappa}^n\Big] \\
& + \frac{e^2}{(q_1+q_2+nk)^2}\frac{g^2}{4\cos^2\theta_W} \\
& \times\Big(\frac{1}{(q_1+q_2+nk)^2 - M_Z^2}\Big) \\
& Tr\Big[(\not{p}_3 + m_\mu)\gamma^\mu(\not{p}_4 - m_\mu)\gamma_\mu(g_v^e - g_a^e\gamma^5)\Big] \\
& \times Tr\Big[(\not{p}_2 - m_e)\kappa^n(\not{p}_1 + m_e)\overline{\tau}^n\Big],
\end{aligned} \tag{22}
$$

where

$$
\begin{aligned}
\tau^n &= C_0B_{0n} + C_1B_{1n} + C_2B_{2n} \quad \text{and} \\
\kappa^n &= D_0B_{0n} + D_1B_{1n} + D_2B_{2n}.
\end{aligned} \tag{23}
$$

The total differential cross section is obtained by summing the partial differential cross section given by Eq. (20) over the possible number of exchanged numbers such that:

$$
\frac{d\sigma}{d\Omega} = \sum_{n\,\text{even}} \frac{d\sigma^n}{d\Omega}. \tag{24}
$$

The calculation of traces that appear in $\left|\overline{M_{fi}^n}\right|^2$ is performed by using FeynCalc Program [40, 41], and the total cross-section is obtained by numerically integrating the Eq. (20) over the solid angle $d\Omega = \sin\theta d\theta d\phi$.

3 Results and discussion

In this section, we present the numerical data obtained by computing the total cross-section of the process $e^+e^- \to \mu^+\mu^-$. Then, we discuss and analyze these results for different laser frequencies and strengths in order to conclude the required and convenient laser parameters. The total cross-section is a summation of partial cross-sections $\sigma = \sum_{n=-\infty}^{+\infty}\sigma^n$. The electromagnetic wave is assumed to be linearly polarized, and its wave vector $\vec{k}$ is considered as co-propagating with the incident beam (e^+e^- beam). The choice of this direction is based on the fact that: In [36], we have studied the laser-assisted muon pair production from e^+e^- annihilation via the exchange of Z and γ bosons. We found that the circularly polarized laser field with a direction perpendicular to the e^+e^- beam reduces the cross section of

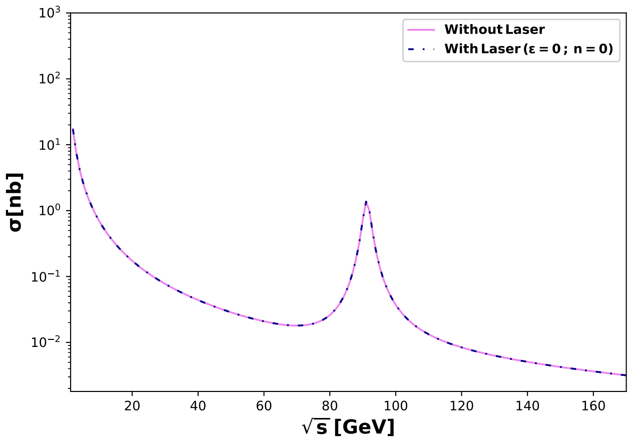

Fig. 2 Comparison between the laser-free total cross-section with laser-assisted total cross-section at the limit of vanishing field $\varepsilon = 0\,V.cm^{-1}$ and $n = 0$

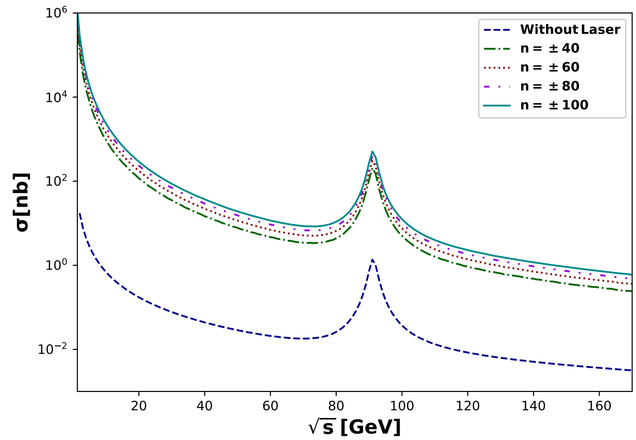

Fig. 3 Dependence of the laser-assisted total cross-section on the centre of mass energy of the collision by considering different ranges of numbers of exchanged photons with $\omega = 1.17\,eV$ and $\varepsilon = 10^5\,V.cm^{-1}$

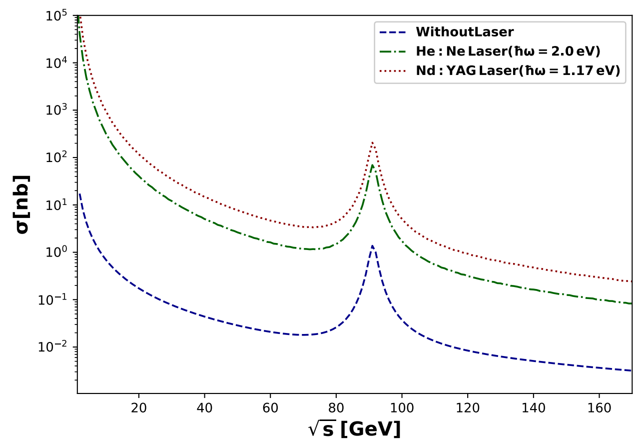

Fig. 4 Variation of the laser-assisted cross-section as a function of $\sqrt{s}$ for different laser sources by fixing their strength at $\varepsilon = 10^5 V.cm^{-1}$ and by summing over n from -40 to $+40$

the process. In [42], we have studied the effect of the direction of the laser field with circular polarization on the cross section of the process. As a result, we found that the circularly polarized laser field that co-propagates with the e^+e^- beam reduces also the cross section. However, the effect of the laser is stronger in this case. In this paper, this is obvious in Eq. (8) where the product $(k.p_i)$ becomes small in the case of e^+e^- traveling in the direction of the laser field. Therefore, the electron/positron will receive an energy increment in the direction of field propagation. Hence, the effect of the laser on the cross section of the process is high. The standard model parameters are chosen such that: the electron mass $m_e = 0.511\,MeV$, the muon's mass $m_\mu = 105.66\,MeV$, the mixing angle $\sin^2(\theta_w) = 0.23126$, the Fermi coupling constant $G_F = 1.1663787 \times 10^{-5}\,GeV^{-2}$, the Z-boson mass $M_Z = 91.186\,GeV$ and its total width $\Gamma_Z = 2.4952\,GeV$ [43]. As a first step in our discussion, we computed the laser-assisted cross section at the limit $\varepsilon = 0\,V.cm^{-1}$ and $n = 0$. Then, we compared it with the total cross section calculated in the absence of a laser field for different centres of mass energies. It is obvious from Fig. 2 that at the limit of vanishing field, the laser-assisted total cross-section tends to the cross-section in the absence of the laser field in all centre of mass energies.

To analyze the effect of the linearly polarized laser field on the total cross-section of the studied process, we show in Fig. 3 the dependence of this cross-section on the centre of mass energy of the collision for a laser field with frequency $\omega = 1.17\,eV$ and strength $\varepsilon = 10^5\,V.cm^{-1}$. According to Fig. 3, we remark that the laser-assisted total cross-section keeps the same behavior as its corresponding laser-free cross-section. For instance, the peak occurs at $\sqrt{s} = M_Z$ (dominance of Z-boson exchange) regardless of the number of exchanged photons. In addition, the γ-photon exchange is dominant at low centre of mass energies. By comparing the laser-assisted cross-section with the laser-free cross-section, it is clear that the total cross-section of the studied process increases inside a laser field with linear polarization. Moreover, its order of magnitude depends on the number of transferred photons between the electromagnetic field and the colliding beam. Indeed, it increases by enlarging the range of exchanged photons numbers. For instance at $\sqrt{s} = M_Z$, the laser-free cross-section is $\sigma \approx 1.4\,nb$. However, the laser-assisted total cross-section, at $\sqrt{s} = M_Z$, can reach $\approx 206\,nb$, $\approx 306\,nb$, $\approx 407\,nb$ and $\approx 508\,nb$ for the number of exchanged photons ± 40, ± 60, ± 80 and ± 100, respectively. Therefore, in the presence of a laser field with linear polarization, the total cross-section of the studied process can be increased by several orders of magnitude.

It is well known that a laser pulse is characterized by its parameters, i.e., its strength and frequency. Consequently, to select the convenient electromagnetic field source, it is worthy to study the variation of the cross-section as a function of the laser parameters. Figure 4 illustrates the variation of the total cross-section as a function of the centre of mass energy for different laser frequencies. Figure 4 shows that the laser-assisted total cross-section of the process $e^+e^- \rightarrow \mu^+\mu^-$ increases as long as the laser frequency decreases for all centre of mass energies $\sqrt{s}$. For instance, at $\sqrt{s} = 60\,GeV$, the total cross-section is $\sigma \approx 0.21\,nb$ in the absence of a laser field, and it is equal to $\sigma \approx 1.62\,nb$ and $\sigma \approx 4.66\,nb$ for $\omega = 2\,eV$ and $\omega = 1.17\,eV$, respectively. Therefore, a powerful laser pulse with low frequency greatly influences the probability of the process to occur compared to laser sources with high frequencies. From the mathematical point of view, the laser field strength contributes to the laser-assisted cross section through the arguments of the generalized Bessel function defined by Eq. (14) and through the A^μ-dependent terms. As the field strength increases up to $\varepsilon = 10^5\,V.cm^{-1}$ (Figs. 3 and 4), the electron state becomes more distorted, and thus the cross section is more strongly modified. Therefore, the cross section increases because the electron's energy increases. Through its propagation inside an electromagnetic field, the charged particle (electron/positron) experiences a ponderomotive energy. The latter is an additive energy to the kinetic energy of the charged particle. Its expression in the presence of a linearly polarized laser field is given by:

$$U_p = \frac{e^2\varepsilon^2}{4m_e\omega^2}. \tag{25}$$

Besides, the number of exchanged photons n has a great contribution to the energy, and this number depends on the frequency of the laser field. This is illustrated in Figs. (3) and (4) where the number of laser photons is high as far as the frequency is small. In addition, the charged fermion (f) acquires an effective mass, m_f^*, inside a linearly polarized laser field such that $m_f^* = \sqrt{m_f^2 + e^2\xi_l^2/2}$ where m_f is its laser-free mass. Each incident particle (electron and positron) will interact several times with the laser field before the electron-positron collision. As a result, the ponderomotive energy and the acquired effective mass of each particle will be multiplied several times. Therefore, we assume that the combination of this laser-acceleration technique with the conventional electron-positron collider will lead to an enhancement of the number of events which is related to the cross section as follows:

$$\frac{dR}{dt} = L \times \sigma, \tag{26}$$

where dR/dt is the number of event per second, L the luminosity of the collider, and σ is the cross section of the particles' interaction. In Fig. 5, the dependence of the cross-section on the laser field strength is shown. In addition, the order of magnitude of this cross-section increases not only

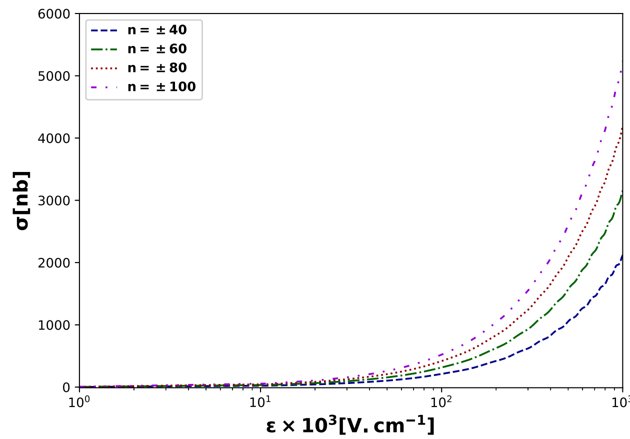

Fig. 5 Dependence of the laser-assisted total cross-section on both laser field strength and number of exchanged photons at the Z-boson pole for $\omega = 1.17\,eV$ and $\sqrt{s} = M_Z$

by increasing the strength of the laser field but also it raises as much as we sum over a large range of exchanged photons number. At $\varepsilon = 10^5\ V.cm^{-1}$ for example, when we sum the partial cross-sections from -40 to $+40$ (-80 to $+80$) the total cross-section is approximately $\sigma \approx 206\,nb$ ($\sigma \approx 407\,nb$). This increase of the cross section is physically justified by the increase in external field photon number density associated with larger values of the laser field strength. The probability that more laser photons will take part in the process also increases.

Figure 6 illustrates the variation of the cross-section of the process $e^+e^- \rightarrow \mu^+\mu^-$ inside a laser as a function of laser strength ε for different laser field sources, i.e., the He:Ne laser ($\omega = 2\,eV$) and the Nd:YAG laser ($\omega = 1.17\,eV$). According to Fig. 6, the laser-assisted cross-section increases as long as we increase the laser field strength, and this confirms the previous results. In addition, this cross-section's order of magnitude increases also as much as the laser field frequency decreases. Physically, the decline of the laser-assisted cross section with increasing laser frequencies is due to the inertia of the electron in responding to the laser-field oscillations, which are caused by the oscillations of the Bessel functions.

The difference between the effects of linearly and circularly polarized [42] laser fields on the behavior of the laser-assisted cross-section can be explained as follows: In a laser wave with circular polarization, the electron moves in perpendicular electric and magnetic fields, and it rotates on an orbit whose radius corresponds to the value of the laser field strength. However, inside a laser wave of linear polarization, the electron moves with linear oscillations in an electric and magnetic field perpendicular to each other, and it does not experience any other movement. Therefore, the probability of electron-positron scattering will be higher inside the linearly polarized laser field than that corresponding to a circularly polarized laser field. The laser technology available

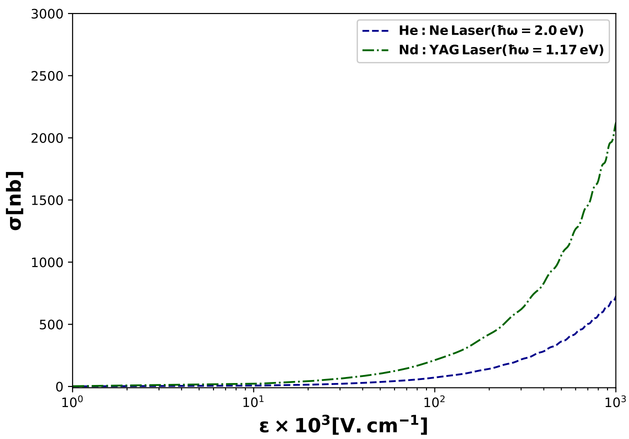

Fig. 6 Laser-assisted total cross-section of the studied process as a function of laser field strength for two different laser fields at $\sqrt{s} = M_Z$ by summing over the number of transferred photons $\boldsymbol{n}$ from -40 to $+40$

today is prominent and very developed. It can provide laser sources with intensities that overcome those presented in the present paper. However, the experimental realization of the studied process is challenging at the present time. This is due to many reasons: The first one is the synchronization of the laser field with the collision time, especially for high energy collisions. The second challenge is about the technical combination of the strong external field with the conventional electron-positron accelerator. Thirdly, the laser pulses that are available today are not short enough, especially for high energy processes. In the atomic physics energy scale, there are many experimental attempts such as Compton scattering and Thomson scattering [44–46]. While the experimental feasibility of the studied process is challenging in the near future, it is interesting to investigate its theoretical framework. In addition, we assume that future particle colliders may offer the opportunity of testing this process.

4 Conclusion

The process of muon pair production in the presence of an electromagnetic field is investigated. The analytic calculation of its cross-section is performed within the S-matrix theory and Dirac-Volkov formalism. The laser wave is assumed to be plane, monochromatic, linearly polarized, and co-propagating with the incident e^+e^- beam. We found that laser wave with linear polarization enhances the total cross-section of the process $e^+e^- \to \mu^+\mu^-$ by several orders of magnitude. In addition, the order of magnitude of the laser-assisted cross-section depends on the laser field parameters. Indeed, a linearly polarized laser wave with strength $\varepsilon = 10^5\ V.cm^{-1}$ and frequency $\omega = 1.17\,eV$ can raise the total cross-section of the studied process at $\sqrt{s} = M_Z$ from $\sigma \approx 1.4\,nb$ (without laser) to $\approx 206\,nb$ by exchanging about ± 40 photons. The most promising setup for an experimental investigation of the process in the near future is based on the combination of a super-intense laser sources with a conventional electron-positron accelerator. We hope that the present work will serve as a stimulus for experimenters to perform such scattering experiments on electrons dressed by a laser wave of linear polarization.

Acknowledgements A special thanks to Mr. Gérald Brun and Mr. Julien Patte for their remarkable work aimed at promoting scientific cooperation with the Moroccan universities. Their dedication and commitment have made a significant impact in strengthening academic ties and advancing scientific research.

Data availability statement No datasets were generated or analyzed during the current study.

References

1. T.H. Maiman, Stimulated optical radiation in Ruby. Nature **187**, 493 (1960)
2. V.I. Ritus, Vacuum polarization correction to elastic electron and muon scattering in an intense field and pair electro and muon production. Nuclear Physics B **44**, 236–252 (1972)
3. Sarah J. Müller, Christoph H. Keitel, Carsten Müller, Higgs boson creation in laser-boosted lepton collisions. Phys. Lett. B **730**, 161–165 (2014)
4. B. Manaut, S. Taj, and Y. Attaourti, Mott scattering of polarized electrons in a strong laser field, Phys. Rev. A **71**, 043401
5. A. Shahbaz, C. Müller, T.J. Bürvenich, C.H. Keitel, Laser-induced nonresonant nuclear excitation in muonic atoms. Nuclear Physics A **821**, 106–117 (2009). https://doi.org/10.1016/j.nuclphysa.2009.02.008
6. P. Francken, C.J. Joachain, Electron - atomic-hydrogen elastic collisions in the presence of a laser field. Phys. Rev. A **35**, 1590 (1987). https://doi.org/10.1103/PhysRevA.35.1590
7. Julio San Roman *et al.*, J. Phys. B: At. Mol. Opt. Phys. **33**, 1869 (2000)
8. S.-M. Li et al., J. Phys. B: At. Mol. Opt. Phys. **35**, 557 (2002)
9. Ai-Hua. Liu, Shu-Min. Li, Jamal Berakdar, Phys. Rev. Lett. **98**, 251803 (2007). https://doi.org/10.1103/PhysRevLett.98.251803
10. M. Baouahi et al., EPL **138**, 14003 (2022). https://doi.org/10.1209/0295-5075/ac63dc
11. M. Baouahi et al., Laser Phys. Lett. **18**, 106001 (2021). https://doi.org/10.1088/1612-202X/ac1e86
12. M. Jakha, S. Mouslih, S. Taj, Y. Attaourti, B. Manaut, Influence of intense laser fields on measurable quantities in W^--boson decay. Chinese Journal of Physics **77**, 1156–1167 (2022). https://doi.org/10.1016/j.cjph.2021.09.011
13. S. Mouslih et al., Phys. Lett. B **833**, 137339 (2022). https://doi.org/10.1016/j.physletb.2022.137339
14. C. Muller, K.Z. Hatsagortsyan, C.H. Keitel, Phys. Rev. D **74**, 074017 (2006). https://doi.org/10.1103/PhysRevD.74.074017. [arXiv:physics/0602106 [physics.atom-ph]]
15. M. Ouali, M. Ouhammou, S. Taj, R. Benbrik, B. Manaut, Laser-assisted charged Higgs pair production in Inert Higgs Doublet Model (IHDM). Phys. Lett. B **823**, 136761 (2021). https://doi.org/10.1016/j.physletb.2021.136761
16. M. Ouhammou, M. Ouali, S. Taj, B. Manaut, Laser-assisted neutral Higgs-boson pair production in Inert Higgs Doublet Model

(IHDM). Chin. J. Phys (2021). https://doi.org/10.1016/j.cjph.2021.09.012
17. S. El Asri, S. Mouslih, M. Jakha, B. Manaut, Y. Attaourti, S. Taj, R. Benbrik, Phys. Rev. D **104**, 113001 (2021). https://doi.org/10.1103/PhysRevD.104.113001
18. Sarah J. Müller, Christoph H. Keitel, Carsten Müller, Higgs boson creation in laser-boosted lepton collisions. Phys. Lett. B **730**, 161 (2014). https://doi.org/10.1016/j.physletb.2014.01.047
19. I. Dahiri, M. Jakha, S. Mouslih, B. Manaut, S. Taj, Y. Attaourti, Elastic electron-proton scattering in the presence of a circularly polarized laser field. Laser Phys Lett. **18**, 096001 (2021)
20. M. Ouhammou, M. Ouali, S. Taj, B. Manaut, Higgs-strahlung boson production in the presence of a circularly polarized laser field. Laser Phys. Lett. **18**, 076002 (2021). https://doi.org/10.1088/1612-202X/ac0919
21. V.I. Ritus, Quantum effects of the interaction of elementary particles with an intense electromagnetic field. J Russ Laser Res **6**, 497–617 (1985). https://doi.org/10.1007/BF01120220
22. A. Di Piazza, C. Müller, K.Z. Hatsagortsyan, C.H. Keitel, Rev. Mod. Phys. **84**, 1177 (2012). https://doi.org/10.1103/RevModPhys.84.1177
23. M. Ouali, M. Ouhammou, R. Benbrik, S. Taj, B. Manaut, Production of Higgs boson in association with a pair of fermions in the presence of a circularly polarized laser field, https://arxiv.org/abs/2204.04563
24. S.P. Roshchupkin, Resonant effects in collisions of relativistic electrons in the field of a light wave. Laser Phys. **6**, 837–858 (1996)
25. S.P. Roshchupkin, A.A. Lebed', E.A. Padusenko, A.I. Voroshilo, Quantum Electrodynamics Resonances in a Pulsed Laser Field. Laser Physics **22**(6), 1113–1144 (2012)
26. S.P. Roshchupkin, A.A. Lebed', E.A. Padusenko, Nonresonant Quantum Electrodynamics Processes in a Pulsed Laser Field. Laser Physics **22**(10), 1513–1546 (2012)
27. N.R. Larin, V.V. Dubov, S.P. Roshchupkin, Resonant photoproduction of highenergy electron-positron pairs in the field of a nucleus and a weak electromagnetic wave. Phys. Rev. A **100**, 52502 (2019)
28. S.P. Roshchupkin, N.R. Larin, V.V. Dubov, Resonant photoproduction of ultrarelativistic electron-positron pairs on a nucleus in moderate and strong monochromatic light fields. Phys. Rev. D **104**, 116011 (2021)
29. S.P. Roshchupkin, A.V. Dubov, V.V. Dubov, S.S. Starodub, Fundamental physical features of resonant spontaneous bremsstrahlung radiation of ultrarelativistic electrons on nuclei in strong laser fields. New J. Phys. **24**, 13020 (2022)
30. S.P. Roshchupkin, A.V. Dubov, S.S. Starodub, The possibility of creating narrow beams of high-energy gamma quanta in the process of resonant spontaneous bremsstrahlung radiation of ultrarelativistic electrons on nuclei in strong electromagnetic fields. Phys. Scr. **97**, 105302 (2022)
31. S.P. Roshchupkin, V.D. Serov, V.V. Dubov, Generation of Narrow Beams of Ultrarelativistic Positrons (Electrons) in the Breit-Wheeler Resonant Process Modified by the Field of a Strong Electromagnetic Wave. Photonics **10**, 949 (2023)
32. S.P. Roshchupkin, S.B. Makarov, Generation of Narrow Beams of Super High-Energy Gamma Quanta in the Resonant Compton Effect in the Field of a Strong X-rayWave. Photonics **11**, 597 (2024)
33. Carsten Muller, Karen Z. Hatsagortsyan, Christoph H. Keitel, Phys. Rev. A **78**, 033408 (2008)
34. Muller, K. Z. Hatsagortsyan, and C. H. Keitel, Phys. Rev. D **74**, 074017 (2006)
35. M. Ouali, M. Ouhammou, Y. Mekaoui, S. Taj, B. Manaut, $Z-$boson production via the weak process $e^+e^- \to \mu^+\mu^-$ in the presence of a circularly polarized laser field. Chinese Journal of Physics (2021). https://doi.org/10.1016/j.cjph.2021.10.007
36. M. Ouali et al., Laser Phys. **32**, 106002 (2022). https://doi.org/10.1088/1555-6611/ac8fe8
37. W. Greiner, B. Mueller, *Gauge Theory of Weak Interactions*, 3rd edn. (Springer, Berlin, 2000)
38. H. R. Reiss, Phys. Rev. A 22, 1786 (1980); 42, 1476 (1990)
39. D.M. Volkov, Z. Phys. **94**, 250 (1935). https://doi.org/10.1007/BF01331022
40. R. Mertig, M. Bohm, A. Denner, FEYN CALC: Computer algebraic calculation of Feynman amplitudes. Comput. Phys. Commun. **64**, 345–359 (1991)
41. V. Shtabovenko, R. Mertig, F. Orellana, Comput. Phys. Commun. **207**, 432–444 (2016). https://doi.org/10.1016/j.cpc.2016.06.008
42. M. Ouali et al., Effect of the laser beam geometry on laser-assisted muon pair production process at e^+e^- collider. Laser Phys. **33**, 016002 (2023)
43. P.A. Zyla et al. (Particle Data Group), Prog. Theor. Exp. Phys. **2020**, 083C01 (2020)
44. T. Kumita et al., Observation of the nonlinear effect in relativistic Thomson scattering of electron and laser beams. Laser Phys. **16**, 267 (2006)
45. D.L. Burke et al., Positron Production in Multiphoton Light-by-Light Scattering. Phys. Rev. Lett. **79**, 1626 (1997)
46. C. Bula et al., Observation of Nonlinear Effects in Compton Scattering. Phys. Rev. Lett. **76**, 3116 (1996)